Deep eye clouds in Tropical Cyclone Trami (2018) during T-PARCII dropsonde observations

Soichiro Hirano[1], Kosuke Ito[1], Hiroyuki Yamada[1], Satoki Tsujino[2], Kazuhisa Tsuboki[3], & Chun-Chieh Wu[4]

[1]University of the Ryukyus
[2]Meteorological Research Institute
[3]Nagoya University
[4]National Taiwan University

Journal of the Atmospheric Sciences, accepted

Typical vertical structure of the eye of tropical cyclones

A skew T–log*p* diagram of the eye sounding for
Hurricane Olivia at 2123 UTC 24 September 1994

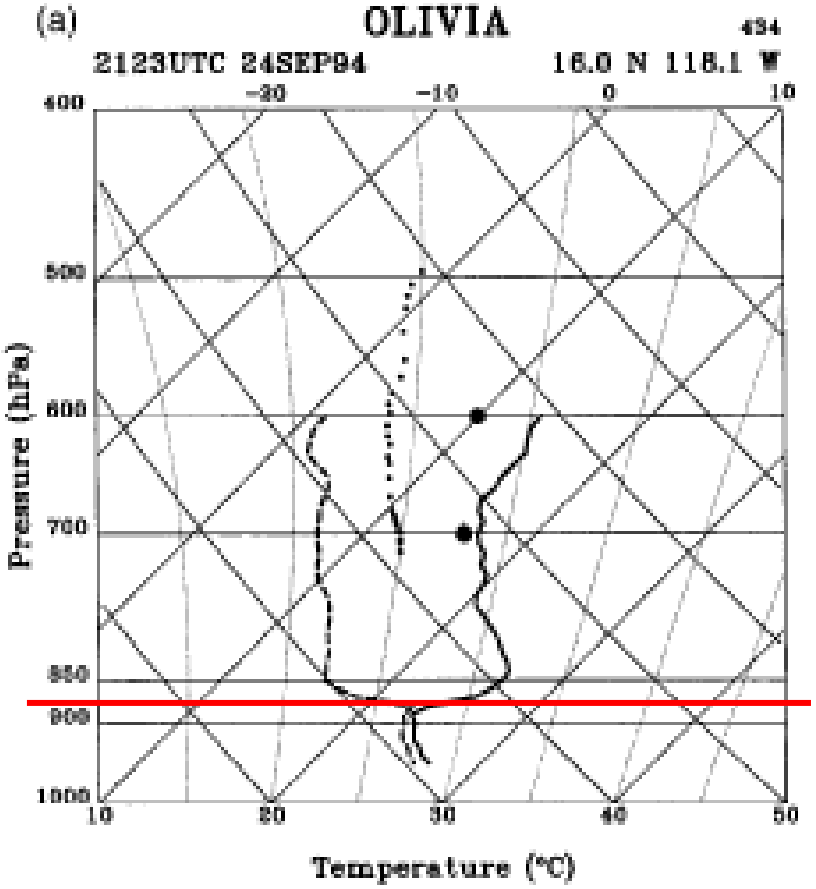

Temperature

Dewpoint temperature

Willoughby (1998)

- The air in the eye of typical intense tropical cyclones (TCs) is separated by a temperature inversion (Jordan 1952; Willoughby 1998; Halverson et al. 2006)
  - Moist, usually cloudy air near the surface
  - Clear, warm, and dry air aloft due to mechanically forced subsidence

Hub cloud

- Hub cloud (Simson 1952; Jordan 1961; Aberson et al. 2006; Schubert et al. 2007)
  - Low-level stratocumulus at the center of the TC eye
  - Surrounded by a(n) (inner) moat of clear air or thin stratocumulus near the outer edge of the eye
  - A larger radius of the eye and smaller Rossby radius of deformation
    ⇒ Concentration of subsidence at the edge of the eye
    ⇒ Favorable condition for the formation of hub clouds at the center of the eye

(Schubert et al. 2007)

The eye of Hurricane Isabel on 13 Sep 2003

Schubert et al. (2007)

Schematic diagram of the eye of Hurricane Edna on 9–10 Sep 1954

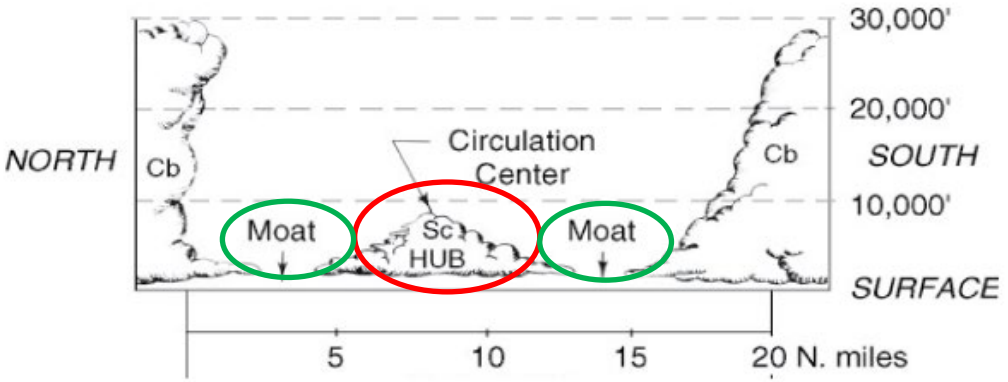

Simson and Starrett (1955)

25 Sep 2018

A photo from the ISS
https://twitter.com/Astro_Alex/status/1044633209454174213/photo/1

26 Sep

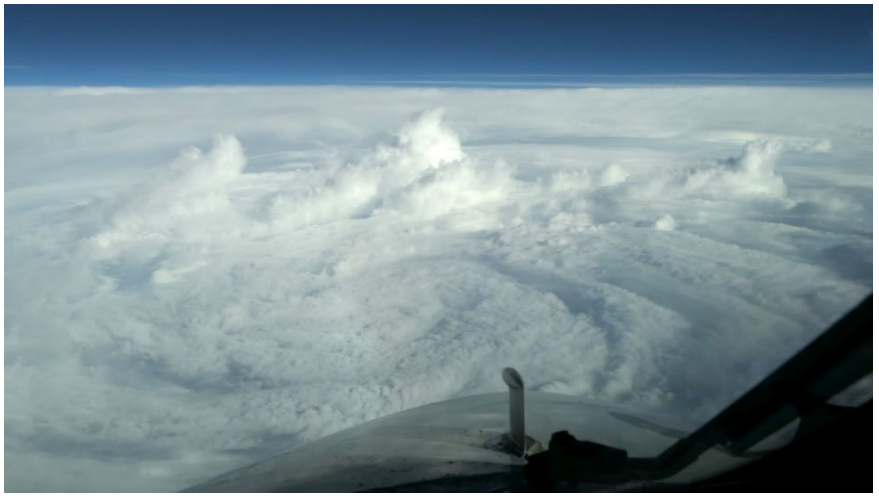

27 Sep

28 Sep

Photos from an aircraft (flight level = 43000 ft or 13.8 km)

Formation of convective clouds in the eye region

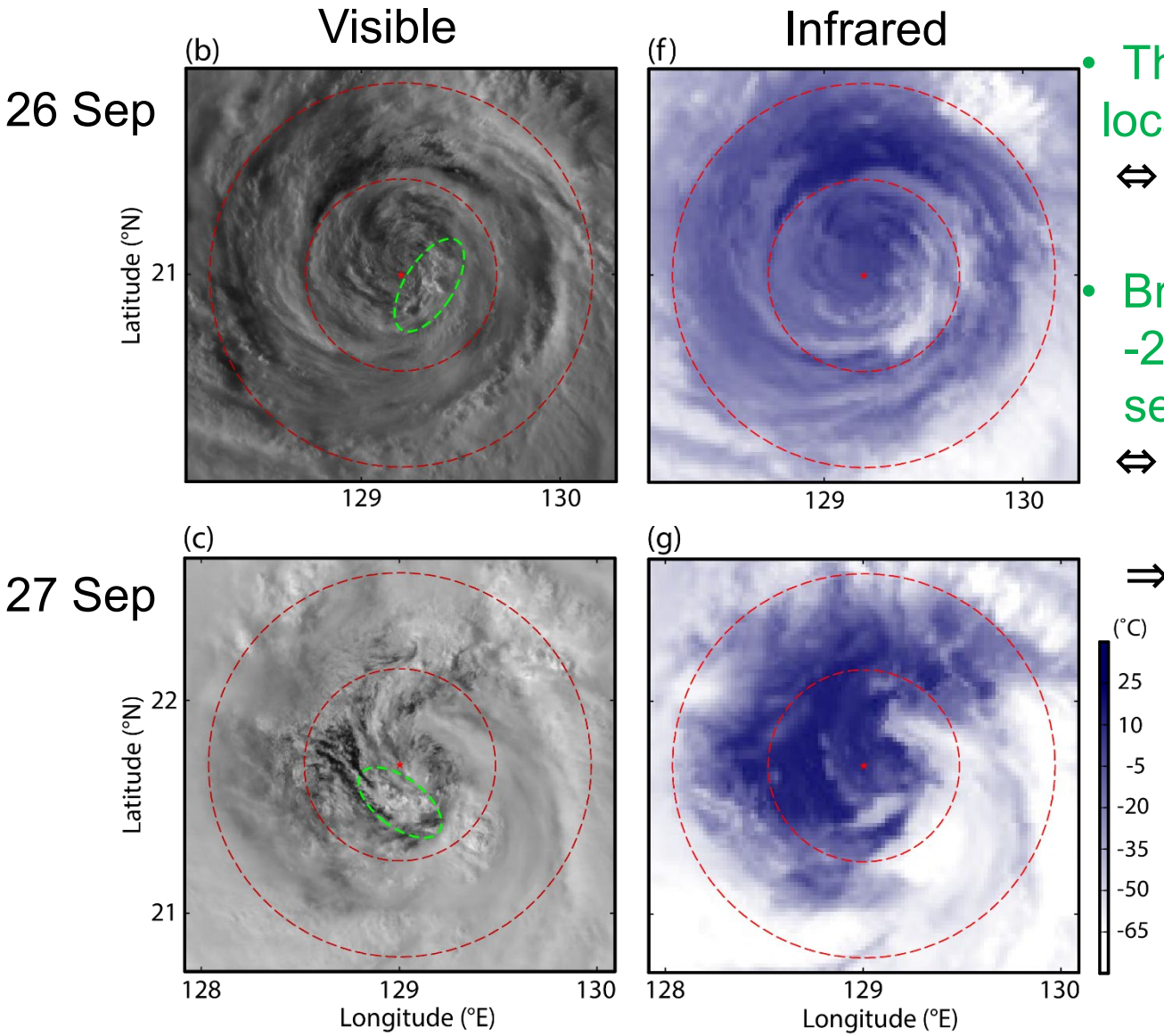

- The convective clouds are located at $10 < r < 30$ km
  ⇔ Hub clouds are located at the TC center.
- Brightness temperature < -20°C (> 9 km above mean sea level)
  ⇔ Top height of hub clouds is approximately 3 km
  ⇒ referred to as <u>deep eye clouds</u>

Almost no previous studies identified deep eye clouds and investigated favorable conditions for their formation.

SST cooling during slow translation of Trami

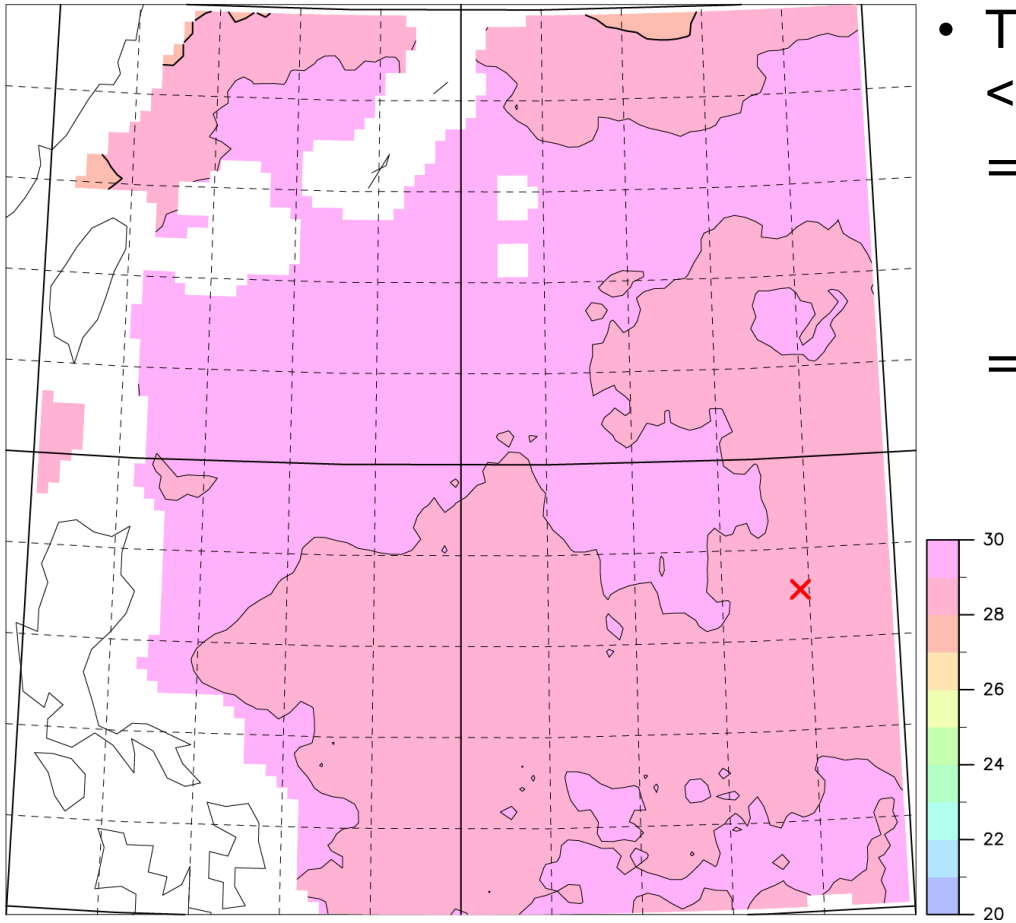

- The translation speed of Trami was < 3 m/s from 25 to 27 Sep

  ⇒ SST cooling caused by three-dimensional process (upwelling) (Yablonsky and Ginis 2009)

  ⇒ *reasonable to use a three-dimensionally coupled atmosphere–ocean model*

× Positions of TC centers from the best-track data from the JMA

The sporadic formation of deep eye clouds is investigated using

- the T-PARCII dropsonde data
- results of a (three-dimensionally) coupled atmosphere–ocean model

Dropsonde observation

- Dropsonde observation from 25 to 28 September 2018 as a part of T-PARCII
  - Horizontal winds, temperature, relative humidity, pressure, (geometric) height, longitude & latitude
  - Dropsondes are launched at an altitude of 43000 ft (13.8 km).
  - Data are obtained at a frequency of 1 Hz.

- Dropsonde data are projected onto radius–pressure cross sections with respect to the TC center from the best-track data.

Paths of dropsondes

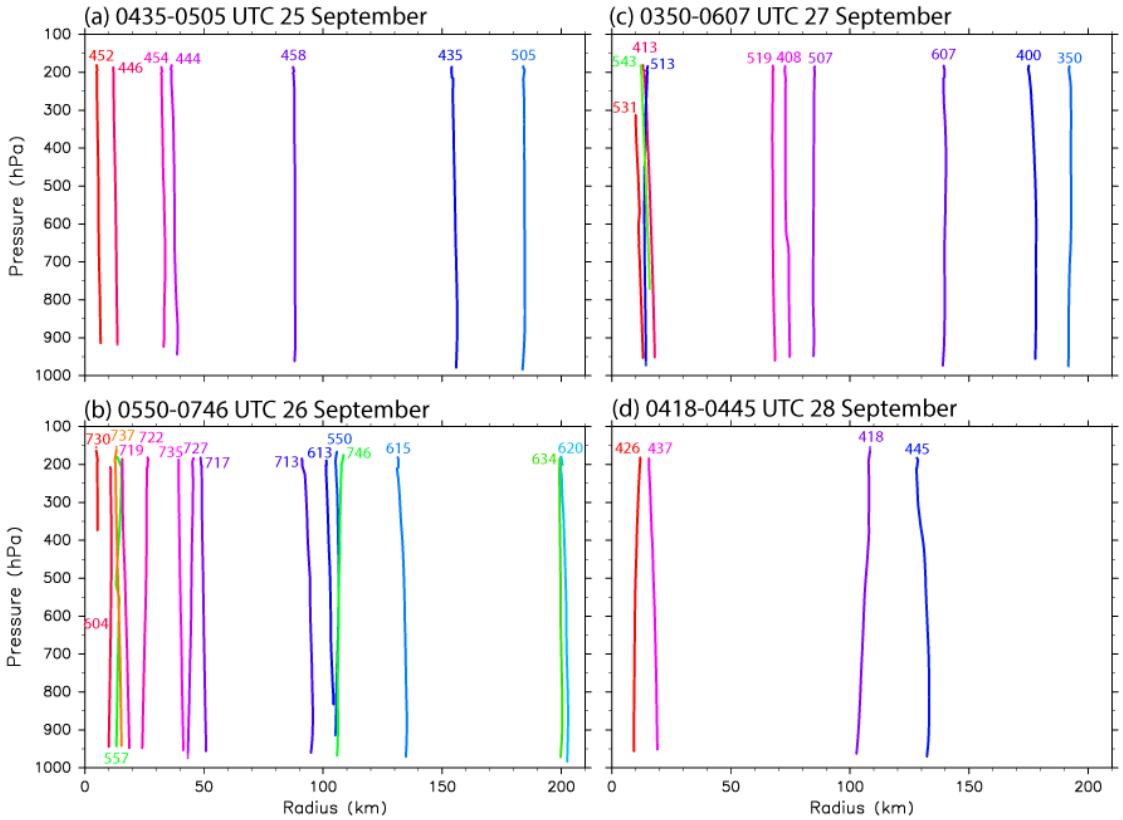

Numerical model settings

- Atmosphere: Japan Meteorological Agency Nonhydrostatic Model (JMA-NHM; Saito et al. 2006; Saito 2012)
  - Horizontal grid spacing: 0.02393° in longitude and 0.02236° in latitude (2.5 km at 20°N)
  - Vertical layers: 30 (–22 km)
  - Time step: 10 seconds
  - Initial date: 22 September 2018

- Ocean: Meteorological Research Institute Community model (MRI.COM; Tsujino et al. 2017)
  - Horizontal grid spacing: 0.1°
  - Vertical layers: 54 (–6000 m)
  - Time step: 300 seconds

An overview of Trami

Central pressures

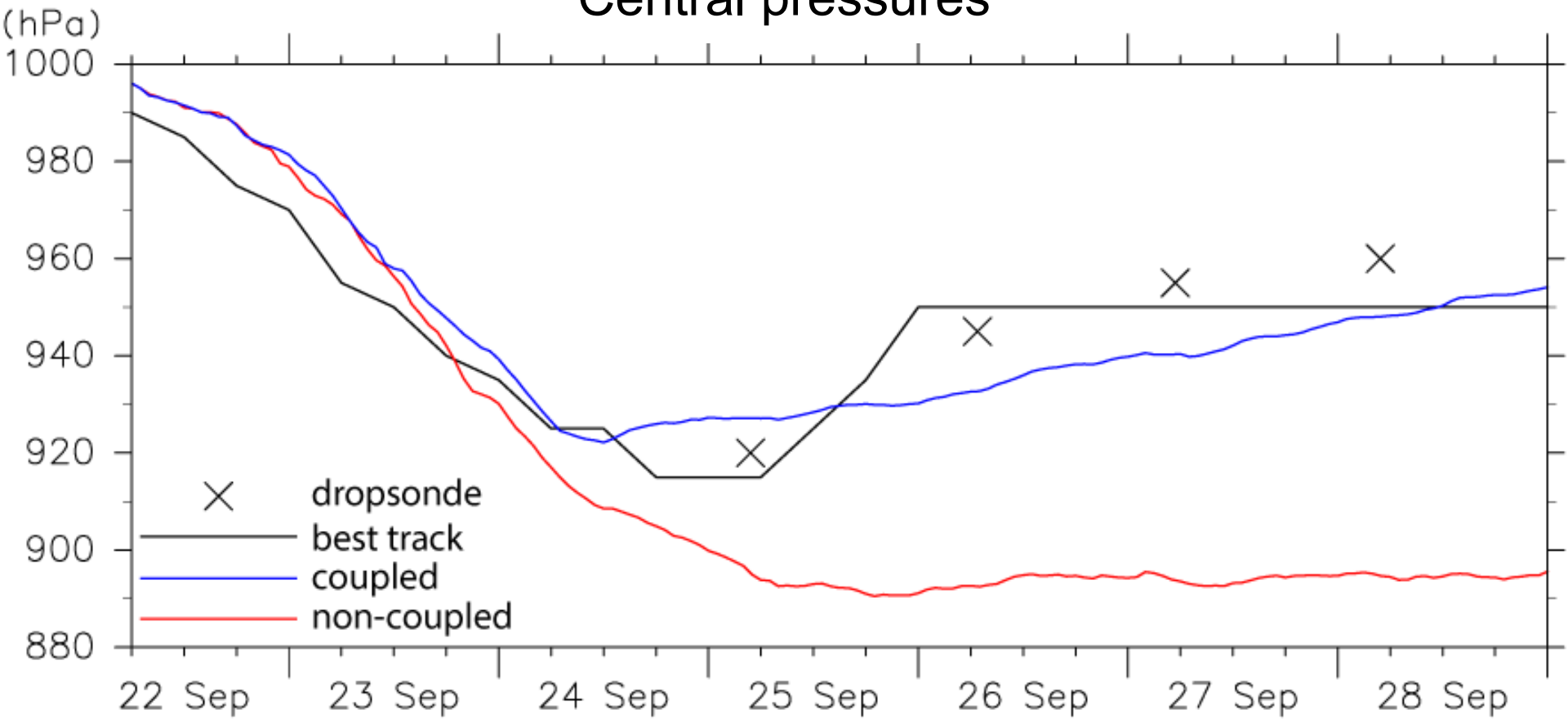

- TC intensity in the coupled model changes similarly to the best track and dropsonde observation.
- A TC in the non-coupled model keeps its intensity after 25 Sep.

An overview of Trami

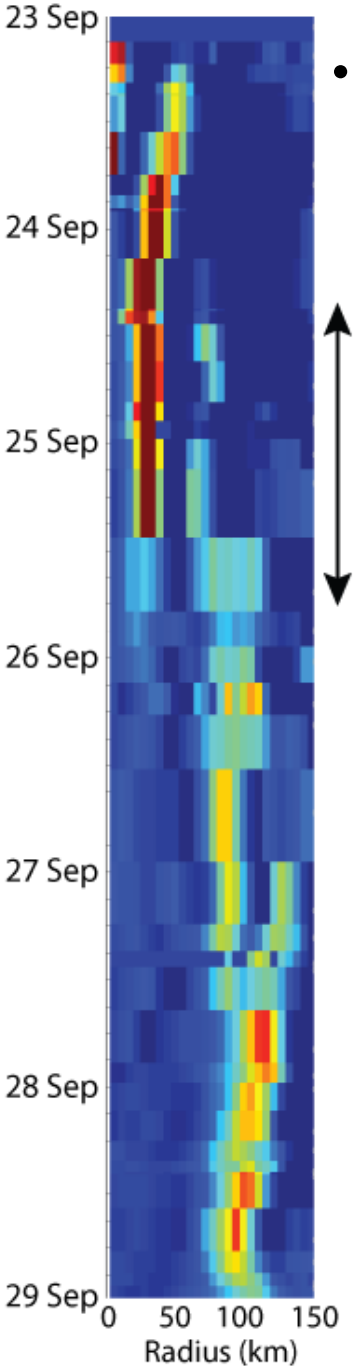

- The ring score
  - Defined based on microwave satellite data
  - Eyewall replacement cycle from 24 to 25 Sep

- Larger radius maximum of wind and weaker tangential wind on 26 Sep than on 25 Sep

Storm-relative tangential wind (dropsonde)

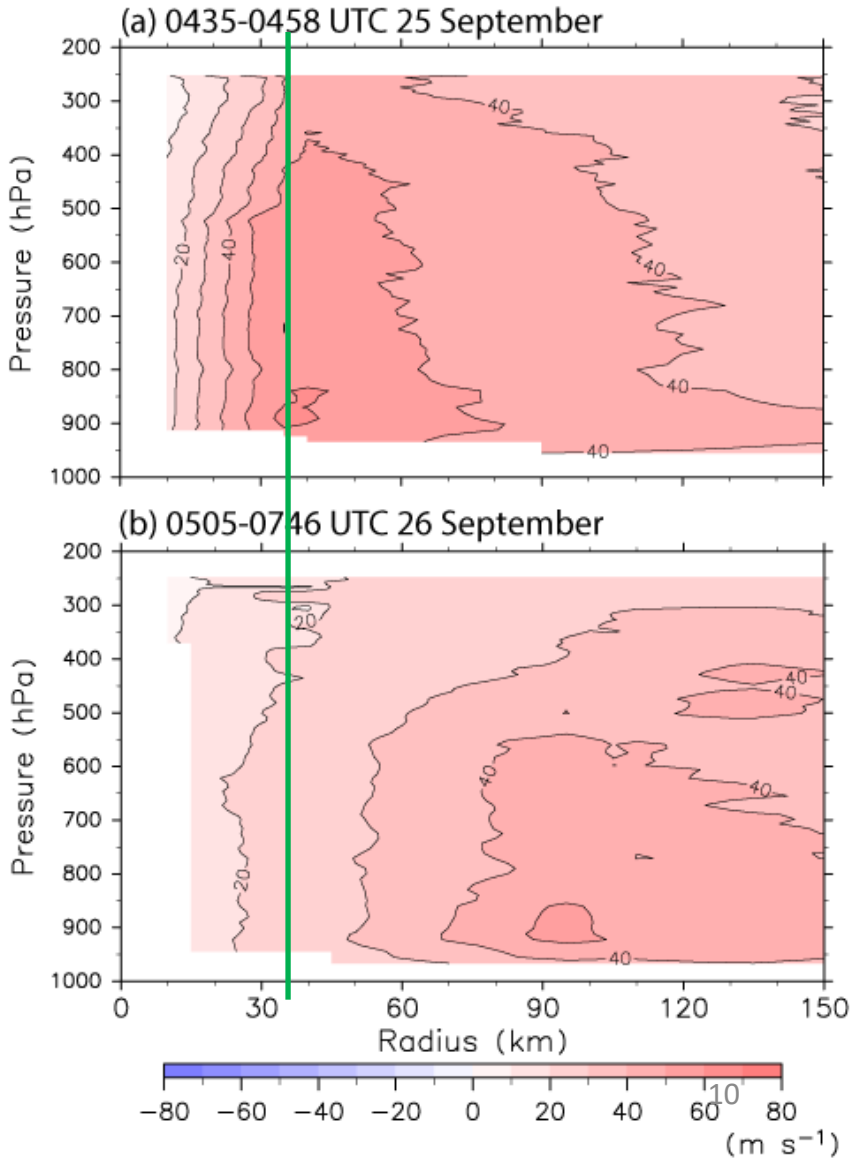

An overview of Trami

Positions of TC centers

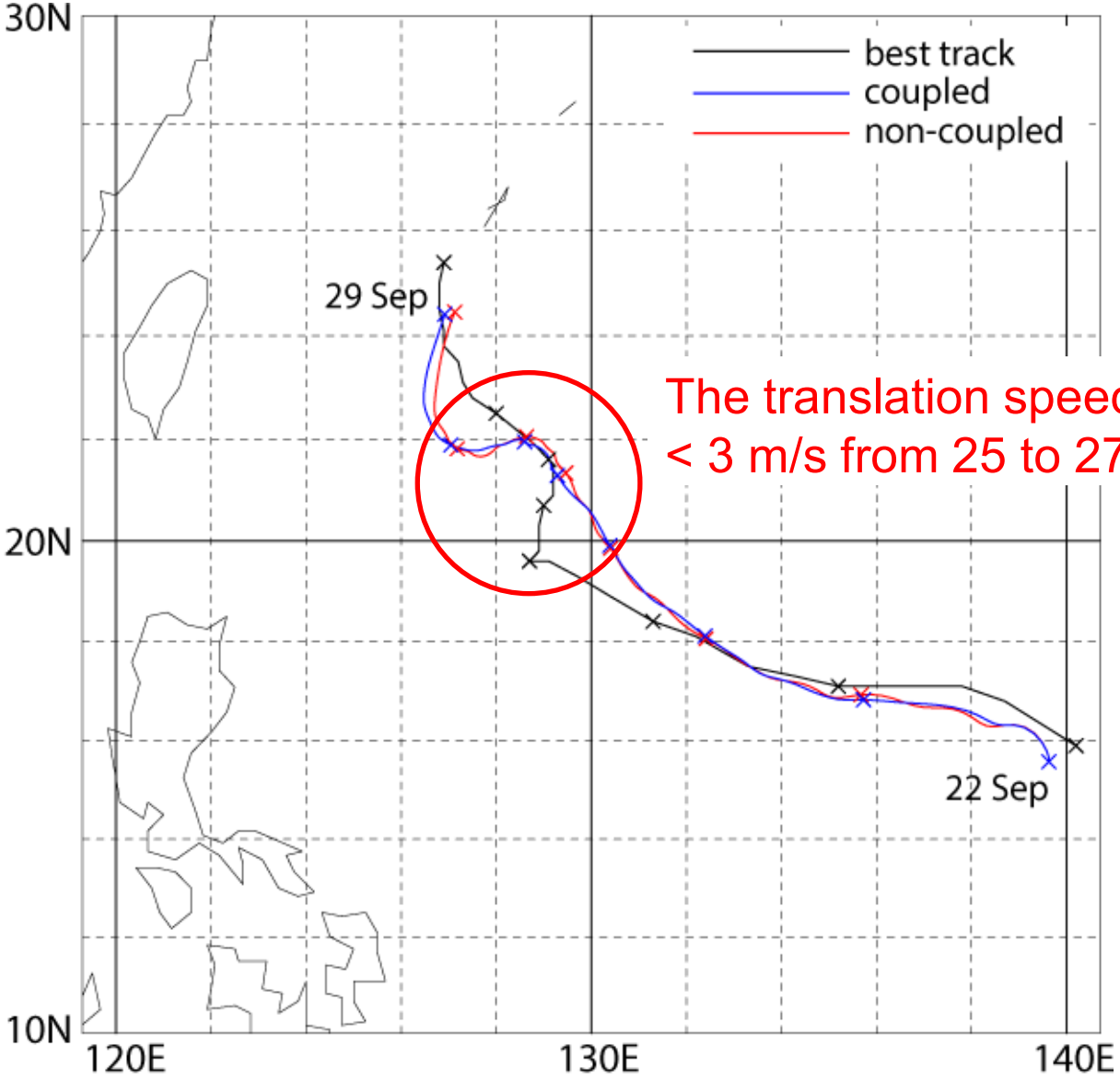

- TCs in both the coupled and non-coupled models follow similar track to the best track data.

Cross marks are plotted at 0000 UTC on each day

Increase in humidity in the eye region

Relative humidity (dropsonde)

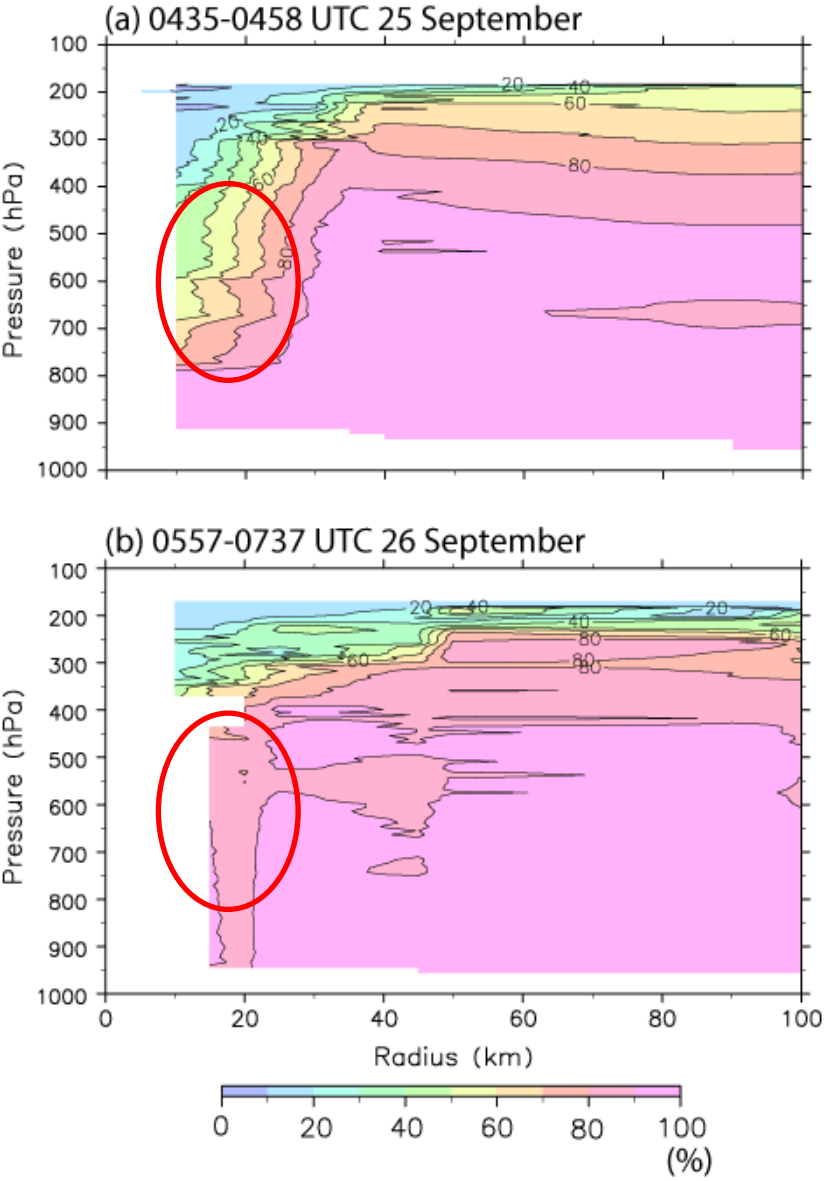

Increase in relative humidity in the eye region from 25 to 26 Sep

- Caused by the sporadic formation of deep eye clouds

The sporadic formation of deep eye clouds in the coupled model

Frequency of total (liquid & ice) cloud water content > 1 mg/kg at 500 hPa (coupled model)

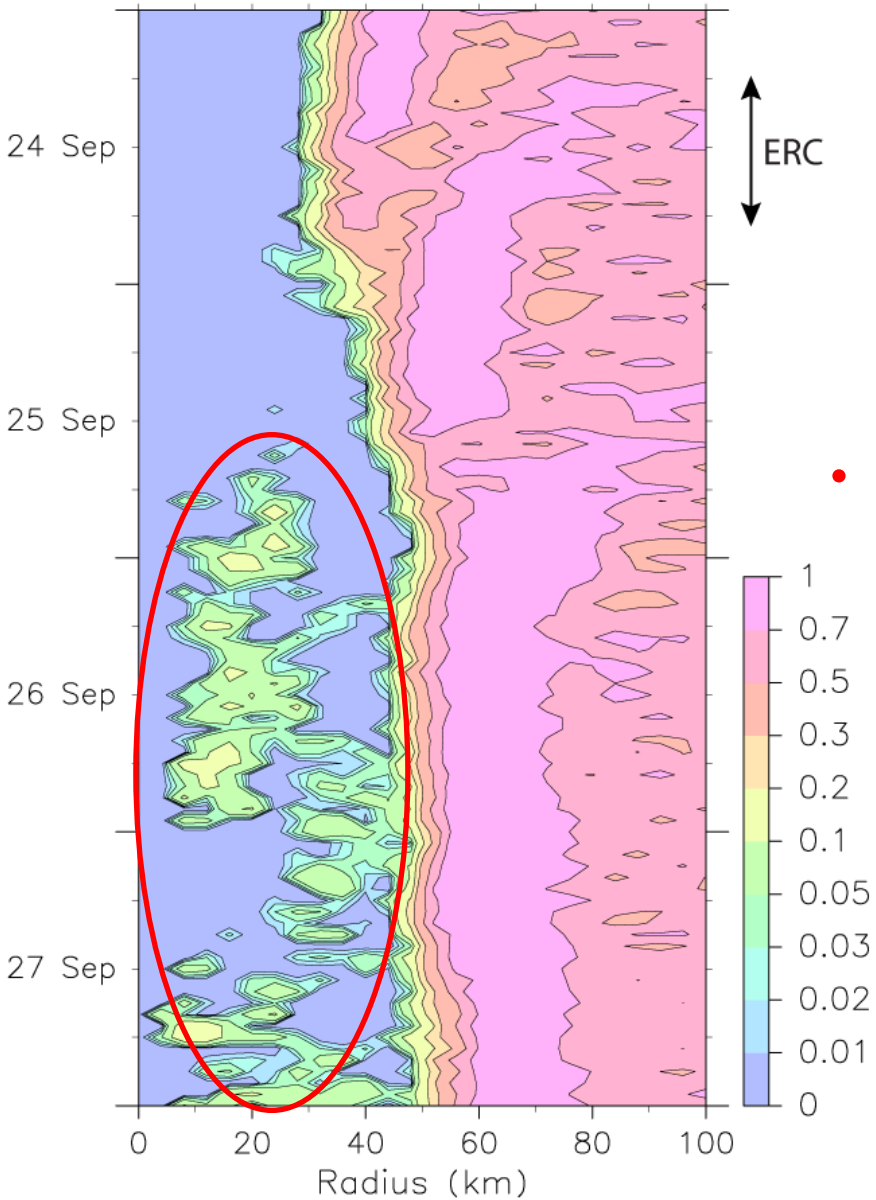

- Emergence of large total cloud water content in the eye region = deep eye clouds

The sporadic formation of deep eye clouds in the coupled model

Total (liquid & ice) cloud water content at 500 hPa (coupled model)

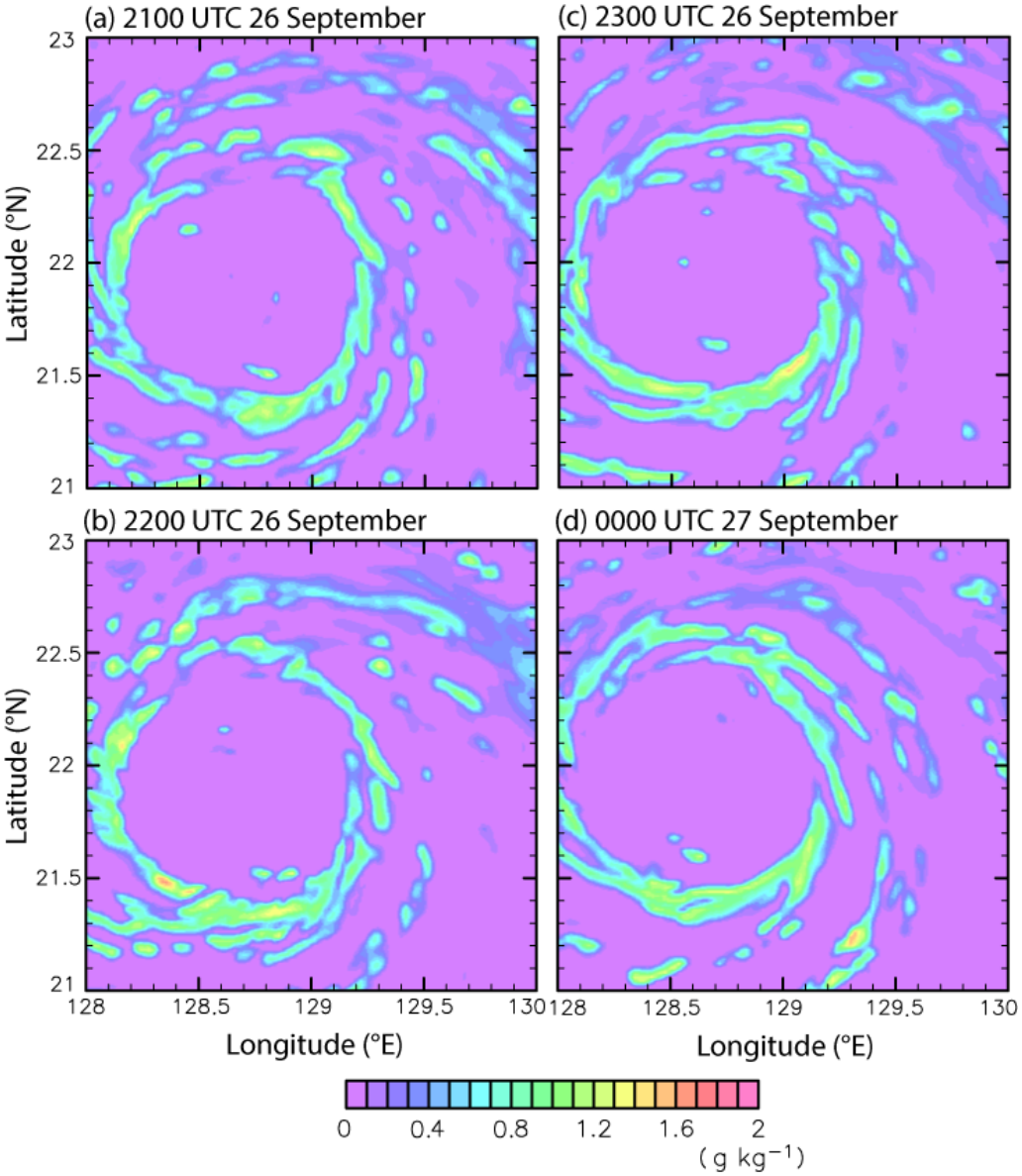

- Sporadic emergence of large total cloud water content in the eye region over a time period of a few hours

The vertical structure of deep eye clouds in the coupled model

Frequency of total (liquid & ice) cloud water content > 1 mg/kg
from 2100 UTC 26 Sep to 0000 UTC 27 Sep
(coupled model)

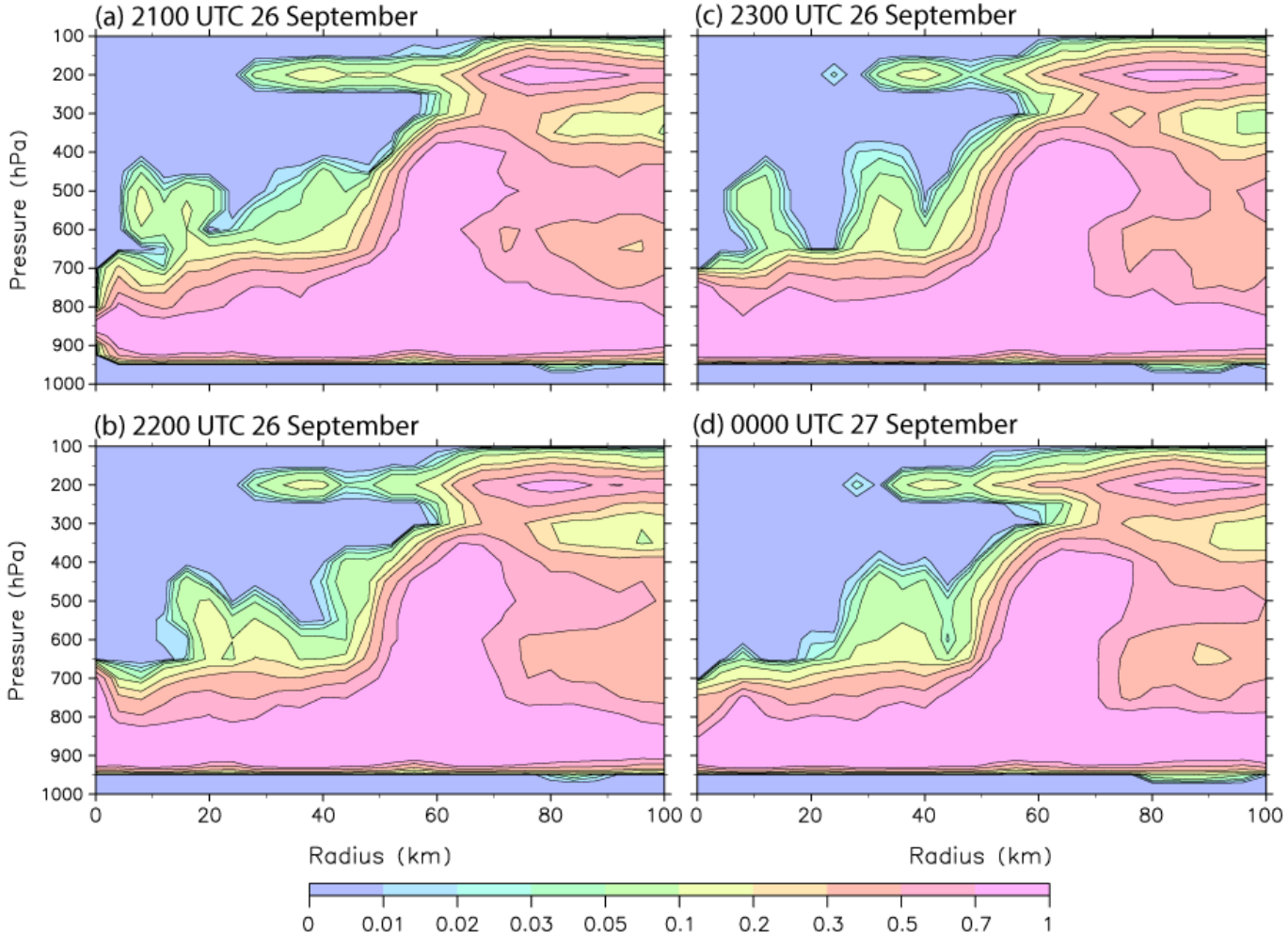

Clouds develop vertically in the eye region over a time period of a few hours.
⇒ Deep eye clouds are reproduced in the coupled model.

Thermodynamic conditions in the eye region

Skew T–log*p* diagrams in the eye region (dropsonde)

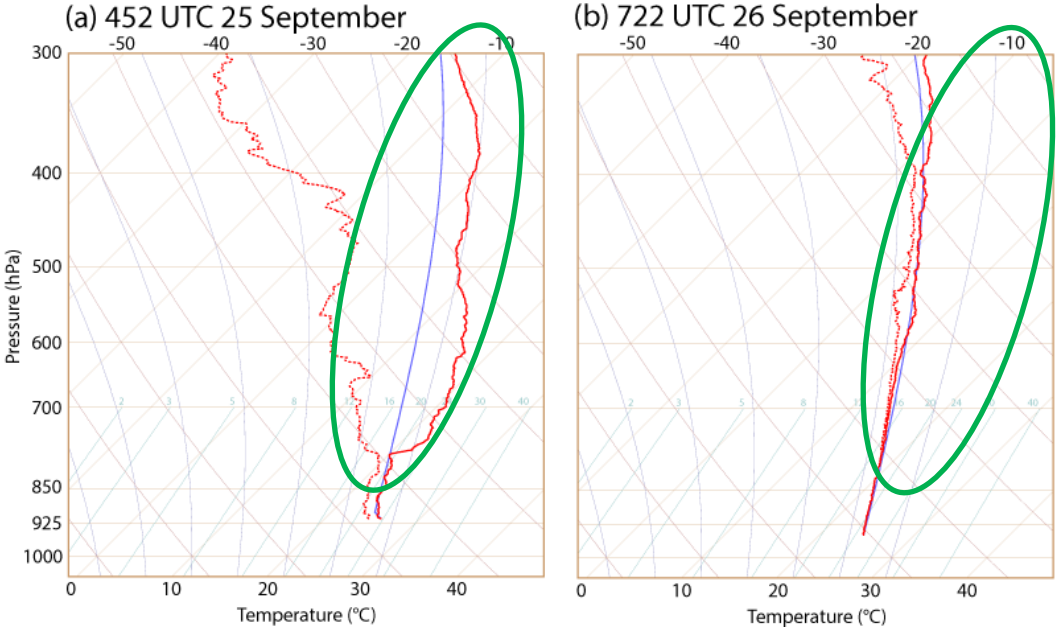

- Temperature
= dew point temperature
= air parcel temperature on 26 Sep
⇒ Consistent with the formation of deep eye clouds
- Temperature decrease from 25 to 26 Sep
⇒ decrease in negative buoyancy
= Favorable condition for convection

Potential temperature anomaly (dropsonde)

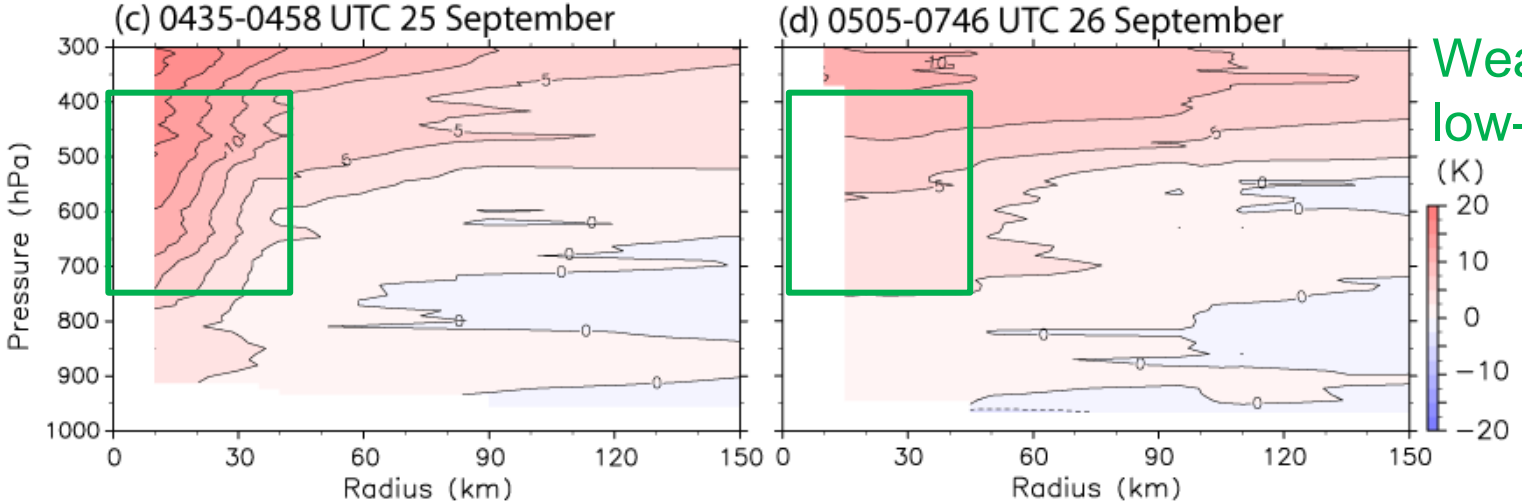

Weakening of a low-level warm core

Vertical motion in the eye region in the coupled model

A histogram of vertical velocity in the altitude range of 600–400 hPa in the eye region in the coupled model

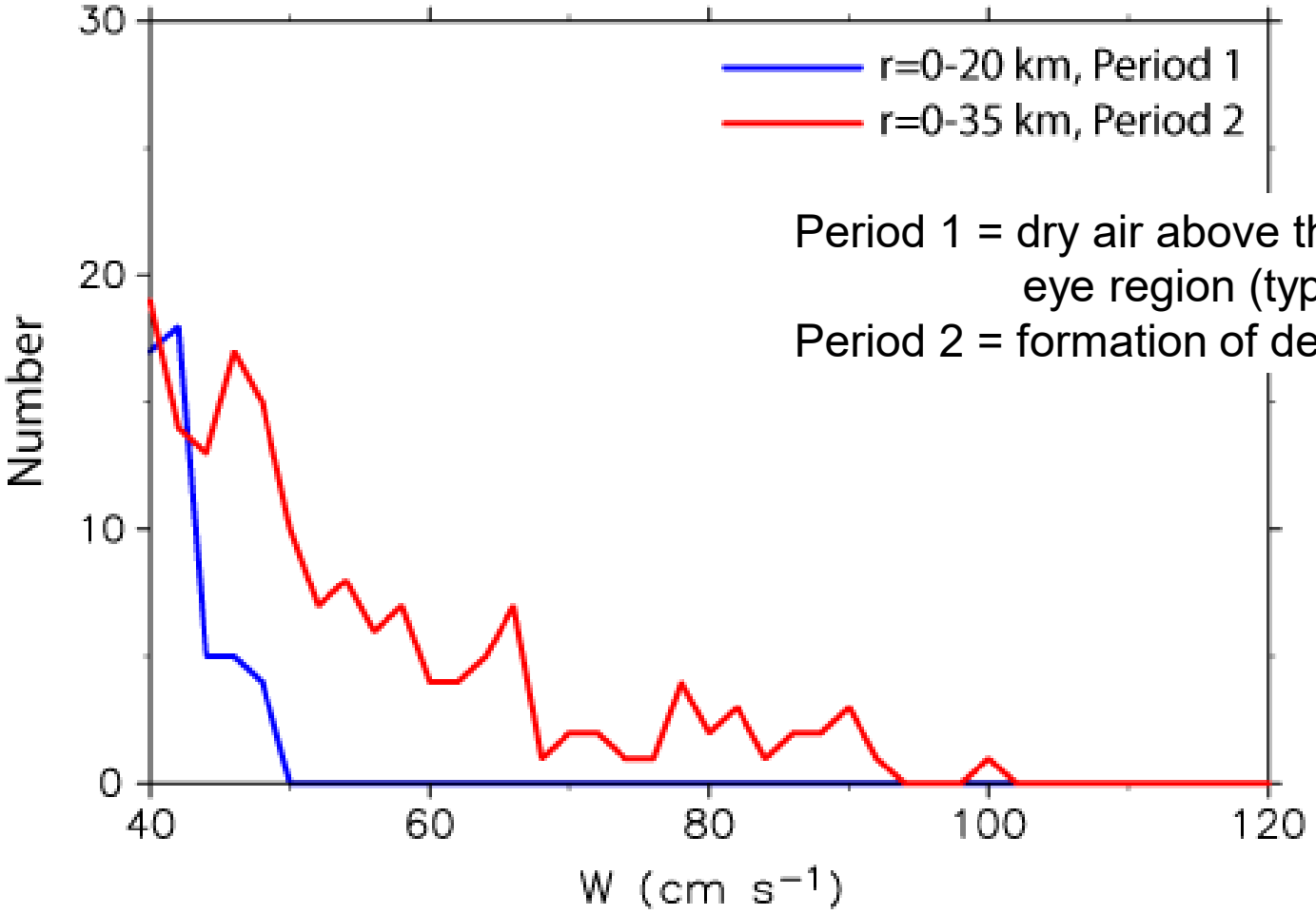

Period 1 = dry air above the inversion in the eye region (typical of intense TCs)

Period 2 = formation of deep eye clouds

Larger frequency of updraft and maximum value of updraft in Period 2 than in Period 1.

⇒ Larger convective activity in the eye region in Period 2

The influence of convective heating within the eyewall on the formation of deep eye clouds

Diabatic heating
in the coupled model

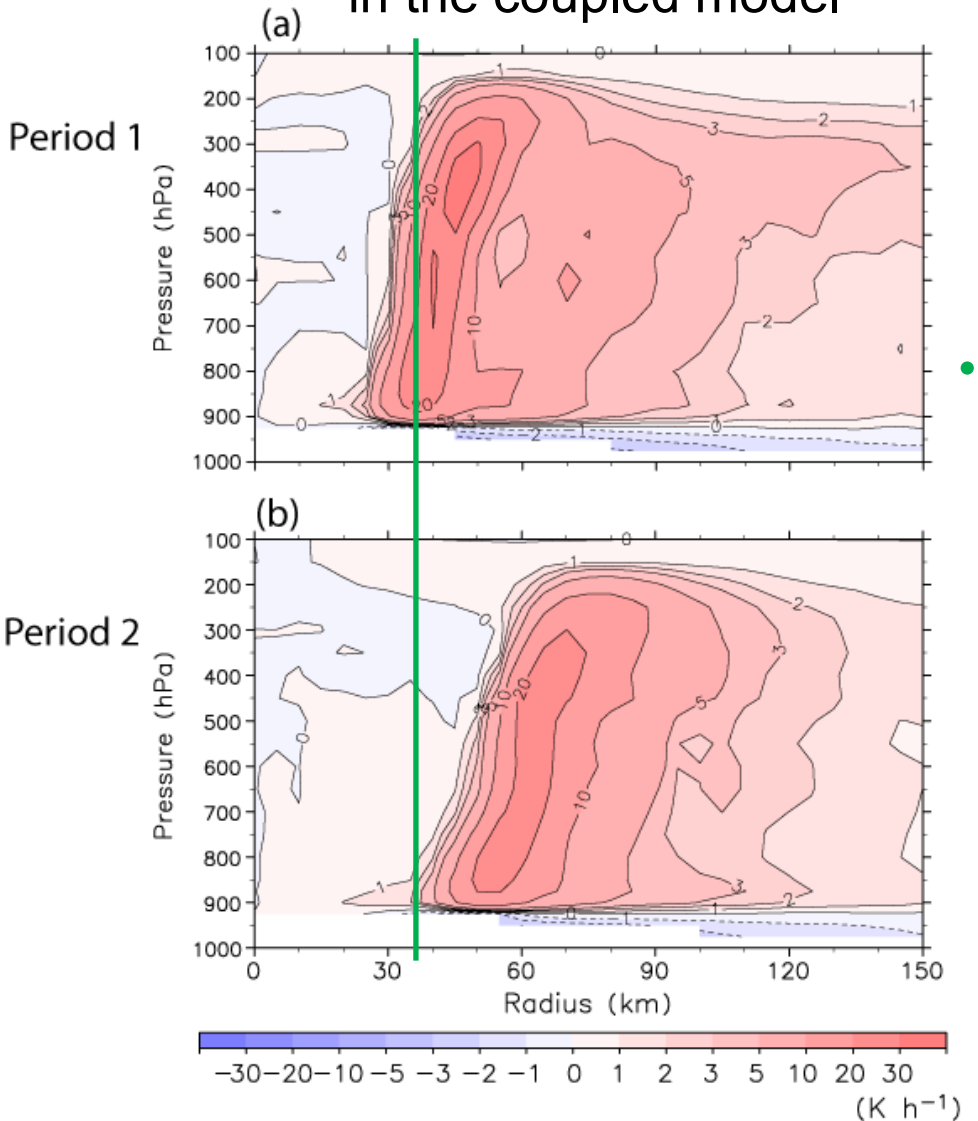

- Outward movement and weakening of diabatic heating within the eyewall from Period 1 to Period 2

The influence of convective heating within the eyewall on the formation of deep eye clouds

Vertical velocity induced by diabatic heating rate > 10 K/h, which is estimated from the Sawyer–Eliassen equation

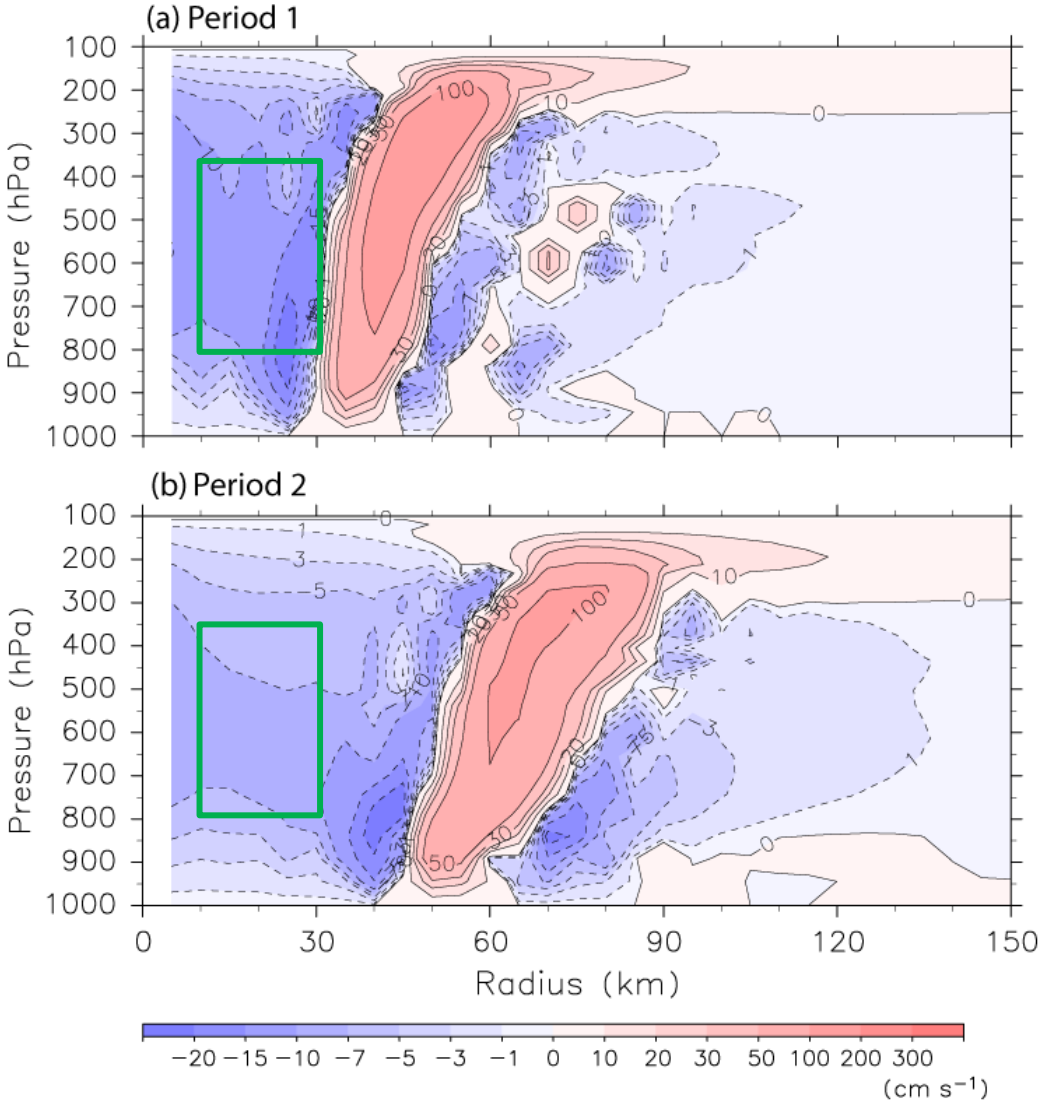

Decrease in downward motion at $10 < r < 30$ km

⇒ Development of frictionally induced ascent to the middle troposphere

⇒ Formation of deep eye clouds

The influence of convective heating within the eyewall on the formation of deep eye clouds

Vertical potential temperature advection induced by diabatic heating rate > 10 K/h at 10 < *r* < 30 km, which is estimated from the Sawyer–Eliassen equation

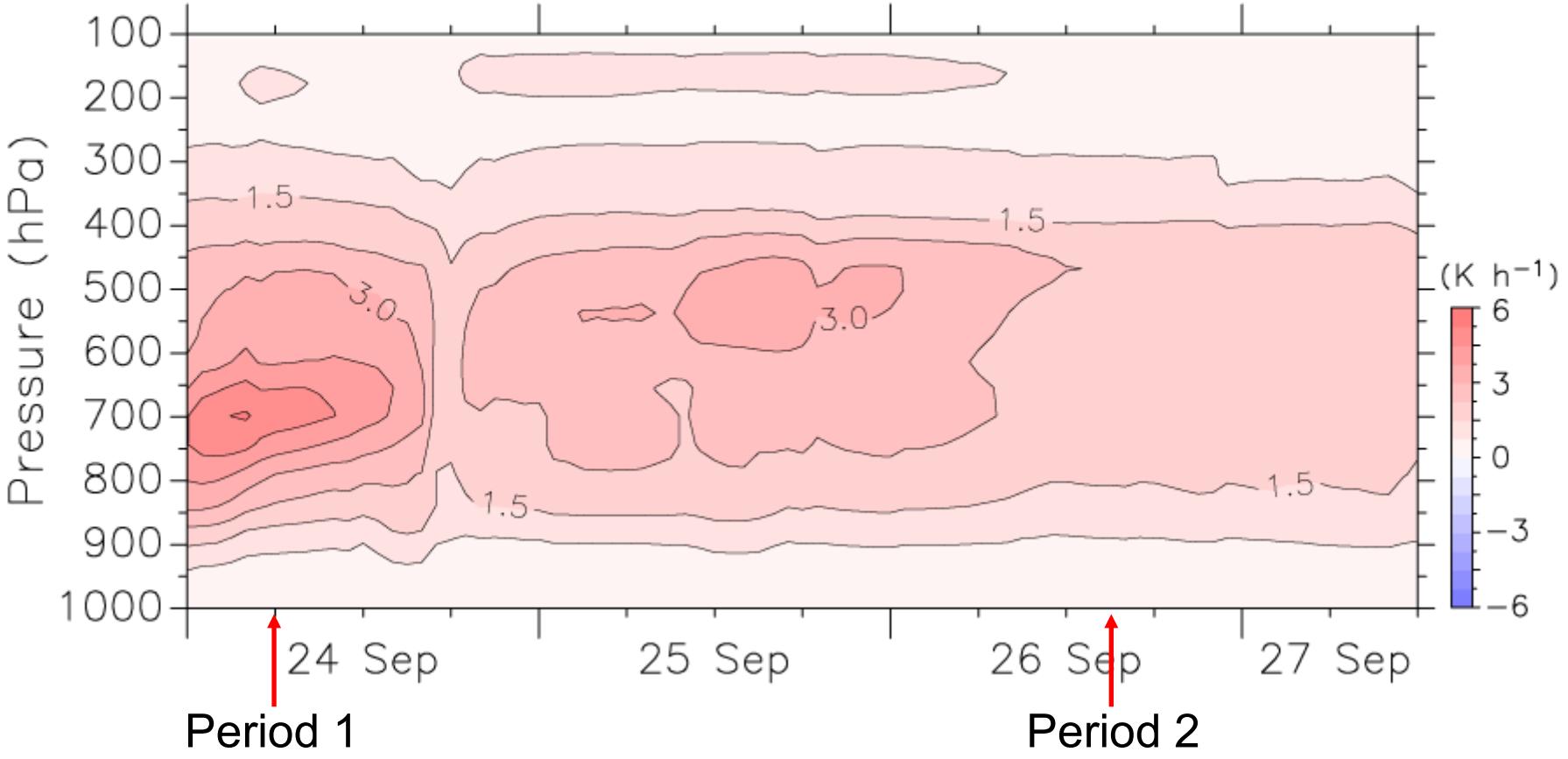

Weaker vertical potential temperature advection in Period 2

⇒ Weakening of the low-level warm core

= Favorable condition for the formation of deep eye clouds

Summary

- The sporadic formation of deep eye clouds in Trami (2018) is investigated using
  - the T-PARCII dropsonde data
  - the simulation results of the coupled atmosphere–ocean model

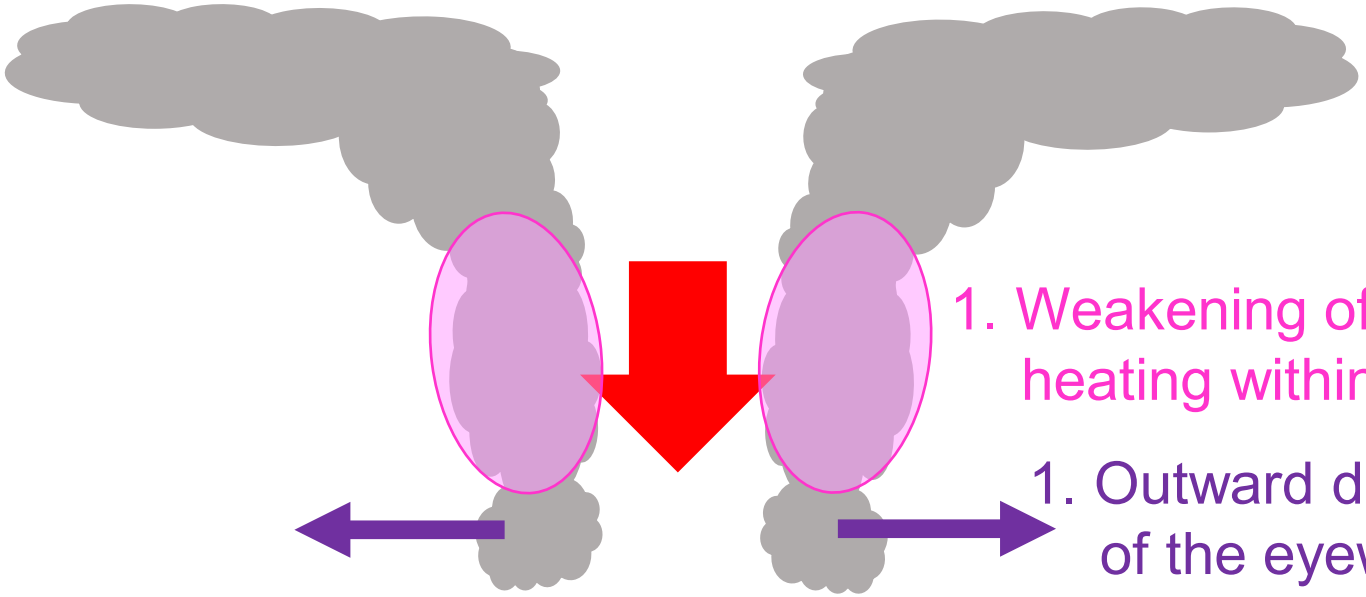

2. Weakening of subsidence and associated adiabatic warming in the eye region

3. Favorable conditions for the sporadic formation of deep eye clouds